

Correction of strong phase and amplitude modulations by two deformable mirrors in a multistaged Ti:sapphire laser

H. Baumhacker, G. Pretzler, K. J. Witte, M. Hegelich, M. Kaluza, and S. Karsch

Max-Planck-Institut für Quantenoptik, Hans-Kopfermann-Strasse 1, D-85748 Garching, Germany

A. Kudryashov, V. Samarkin, and A. Roukossouev

Adaptive Optics for Industrial and Medical Applications Group, Institute on Laser and Information Technology of the Russian Academy of Science (ILIT RAS), Svyatoozerskaya Street 1, Shatura, Moscow Region, 140700 Russia

Received May 23, 2002

We describe a novel scheme consisting of two deformable bimorph mirrors that can free ultrashort laser pulses from simultaneously present strong wave-front distortions and intensity-profile modulations. This scheme is applied to the Max-Planck-Institut für Quantenoptik 10-TW Advanced Titanium-Sapphire Laser (ATLAS) facility. We demonstrate that with this scheme the focusability of the ATLAS pulses can be improved from 10^{18} to 2×10^{19} W/cm² without any penalty in recompression fidelity. © 2002 Optical Society of America
OCIS codes: 010.1080, 140.3590, 220.1000.

In high-power multistage Nd:glass and Ti:sapphire (TiS) laser systems, wave-front aberrations (WFAs) that result in deterioration of beam quality are common. These WFAs originate from imperfections in the many optical components that are present in the beamline as a result of optical figure errors, pump-induced thermal distortions in the amplifiers, and the third-order nonlinear n_2 effect. In TiS lasers, cooling the crystals to the temperature of liquid nitrogen can essentially eliminate pump-induced distortions.^{1–3} A more versatile approach, however, is to use adaptive optics, which can counteract each of the three WFA sources, regardless of whether they occur individually, in pairs, or all together simultaneously. This was demonstrated in Refs. 4–7 by use of just a single deformable mirror (SDM).

In the SDM concept, only the WF of the pulse is corrected, not the intensity profile. This scheme works well as long as the WF perturbing action of each individual optical element is so weak that the shortest local radius of curvature, R , of the WF of the exiting pulse is many times the distance to the adaptive mirror. In addition, the pulse should not pick up strong intensity modulations, e.g., by nonuniform amplification. However, when an optical element such as a multipass amplifier causes a single-pass WFA with an associated R value of the order of the pass-to-pass propagation distance, the pulse intensity profile becomes increasingly modulated from pass to pass. On further propagation, these modulations may get even worse. If one stays with the SDM concept, the beam loading would then have to be reduced so that the optical components placed downstream from the amplifier are not damaged. In chirped-pulse amplification laser systems, the compressor gratings are then particularly endangered because of their low damage threshold. The system efficiency is thereby decreased considerably, too.

In this Letter we study this heavy-perturbation case, which to our knowledge has not been investigated experimentally before and is characterized here by the simultaneous presence of strong phase and amplitude modulations. We show that by invoking two DMs one can cancel the modulations without any sacrifice

in beam loading. In our concept, the compressor is placed between two DMs and thus has to be operated with a distorted WF. For this situation, we present conditions that, when met, maintain the pulse recompressibility and focusability within reasonable limits.

The two-DM concept has also been investigated for applications in areas others than the one studied here, so far only theoretically. These other applications include beam shaping for high-power laser beams in laser photochemistry and material processing⁸ as well as delivering a high-quality pulse on a remote target after propagation through turbulent atmosphere.⁹ In astronomy, the use of two DMs may enable one to overcome turbulence-induced phase and amplitude modulations for widely enlarged fields of view (Refs. 10 and 11, and references therein). The algorithms developed in Refs. 8–11 for control of the DM surfaces are not applicable to our situation because of the presence of the gratings between the two DMs, which limits beam loading.

The heavy-perturbation case that we are confronted with arises in the final disk amplifier of our Advanced Titanium:Sapphire Laser (ATLAS) facility (Fig. 1). The front end of the laser¹² delivers a 300-mJ pulse that is centered at 790 nm and stretched from 100 fs to 200 ps with a smooth intensity profile and a well-behaved WF. After four passes, the fluence pattern of the pulse inside the compressor is heavily modulated (Fig. 2, left) due to crystal-growth defects (Fig. 3) and pump-induced aberrations. At a pulse energy of 1.3 J at the compressor entrance, the peak fluence reaches 0.3 J/cm² on the first grating, far beyond its damage threshold of 0.15 J/cm². Under these loading conditions, the energy that is transmittable through the compressor is limited to only 0.5 J. Because of the simultaneous presence of WFAs and intensity modulations, the SDM concept is no longer applicable. To increase the amount of energy that is transportable through the compressor, we must first smooth the fluence profile. This is achieved with deformable mirror DM1 (17 electrodes, 30-mm diameter, bimorph),¹³ which replaces the plane mirror in the beamline before the pulse makes its final transit through the amplifier

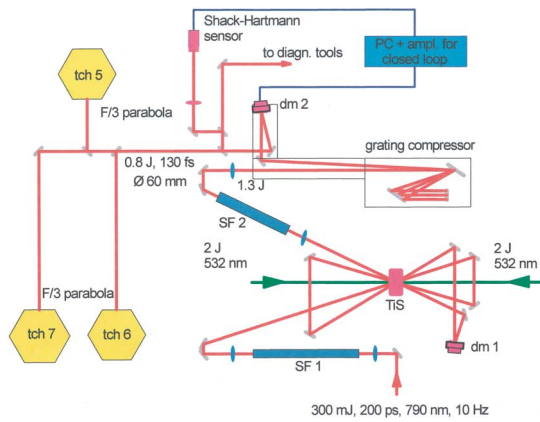


Fig. 1. Setup of the final amplifier in the ATLAS facility with two deformable mirrors, DM1 and DM2, closed loop, and three target chambers (TCH5–TCH7). The TiS crystal of 40-mm outer diameter is pumped from two sides. The TiS pulse provided by the front end passes through the crystal four times and is thereby amplified from 0.3 to 1.5 J. The pulse then runs through spatial filter SF2, and the pulse diameter increases from 18 to 63 mm. The pulse is then recompressed to 130 fs in an evacuated compressor chamber that houses two holographic gold gratings and is connected to the target chambers by evacuated tubes.

(Fig. 1). The best electrode voltage settings for DM1 can be found manually with a few iterations by use of a real-time beam-profile analyzer. For the same energy of 1.3 J as before, the peak fluence of the smoothed profile is then reduced to 90 mJ/cm^2 so that the 1.3-J energy can be safely transmitted through the compressor. At constant voltage settings, the smoothed beam profile remains stable over weeks and changes little on propagation inside the compressor and a few meters downstream.

The action of DM1 modifies the WFAs originating in the amplifying crystal but does not generate a plane WF. A plane WF is generated with a second deformable mirror, DM2 (33 electrodes, 80-mm diameter, bimorph).¹³ DM2 is placed behind the compressor so that it is able to compensate for the optical figure errors of the gratings and to ensure that highly peaked intensity patterns that might occur when DM2 is optimized cannot damage the gratings. The compressor is thus fed with a chirped pulse whose WF is distorted. In this situation, which was investigated theoretically in Ref. 14, the following three effects are of major importance: loss of compression fidelity, astigmatism, and chromatic aberration. For an estimate of the level of WFAs that are tolerable without too high a loss in beam quality, the rigorous theory¹⁴ is not needed. It is sufficient to replace the real pulse with a spherical WF whose curvature is chosen to be equal to the maximum local curvature in the real distorted WF. The focus of the model WF is downstream DM2.

From measurements, we find that the recompression fidelity in terms of pulse duration and contrast is hardly affected as long as any local radius of curvature of the WF exceeds 15 m. The condition is met in the ATLAS for pulse energies of up to 1 J after compression.

The originally spherically convergent beam turns astigmatic when it leaves the compressor, leading to the occurrence of two focal lines instead of a single point focus because the beam behaves differently in the dispersion and nondispersion planes of the compressor. With $R \geq m$, the compressor-induced astigmatism turns out to be weak and is hence easily correctable with DM2, since the necessary displacement is $\leq 1 \mu\text{m}$. The compensation of the original beam compression is not a problem, either.

The chromatic aberration originates from the different path lengths of the individual spectral components on their way through the compressor. When they are exiting, the individual spectral beam components still have the same cone angle, but at a fixed position in space the radii of curvature are different. This effect cannot be compensated for with DM2. The beam emerging from DM2 will hence be parallel for the spectral component near λ_0 but divergent for the components with $\lambda < \lambda_0$ and convergent for those with $\lambda > \lambda_0$. The focus of such a beam is hence no longer pointlike but exhibits longitudinal spreading, with each spectral component having its own focus located at a different position. This spreading is tolerable when the foci of all colors inside the spectral range $4\Delta\lambda_{\text{FWHM}}$ lie within the Rayleigh length of the spectral beam component at λ_0 . For the ATLAS, this criterion requires $R > 15 \text{ m}$, which is met. The theoretical analysis reveals that $R \propto \Delta\lambda_{\text{FWHM}}$. Very short pulses with $\Delta\lambda_{\text{FWHM}} \geq 50 \text{ nm}$ thus need to be rather well collimated if one wishes to avoid intensity degradation in the focus. This conclusion is in fair agreement with the results of the rigorous theory.¹⁴

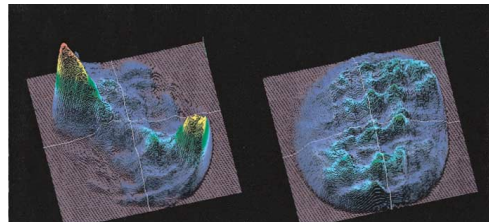


Fig. 2. Fluence patterns in the plane of the first compressor grating. Left, DM1 is replaced with a plane mirror; peak fluence, 300 mJ/cm^2 . The double-peak pattern is due to the coarse two-half structure of the WFAs shown in Fig. 3. Right, DM1 is optimized; peak fluence reduced to 90 mJ/cm^2 . The remaining fluence modulation arises from the fine structure of the WFAs (Fig. 3). The very high spatial frequencies, which carry little energy, are lost on propagation through the spatial filter SF2 (Fig. 1).

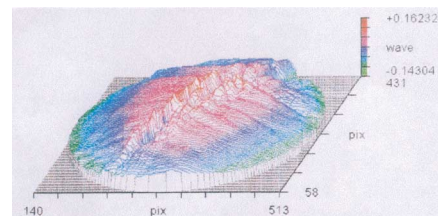


Fig. 3. WFAs that are due to growth defects in the final disk amplifier of 40-mm diameter, 17-mm thickness, and $\alpha l = 2.3$ at 532 nm.

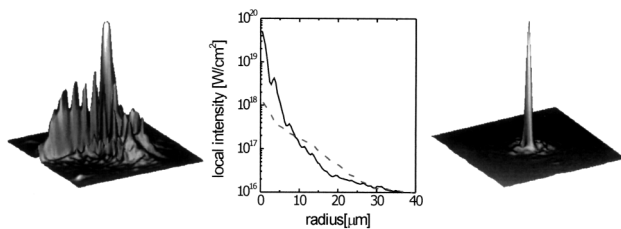


Fig. 4. Fluence profile in the focus of the $F/3$ off-axis parabola. Left, DM1 and DM2 are on, but DM2 acts as a plane mirror. Middle; local intensity as a function of radius for the fluence profiles shown to the left (---) and right (—). Right, DM1 and DM2 are on, but DM2 is locked to operation for minimal WFAs.

We generate a parallel beam with DM2 by comparing the actual WF as measured with a Shack–Hartmann sensor that has a 12×12 lenslet array with a reference WF obtained from a diode laser running at 790 nm and expanded to a parallel beam of 63-mm diameter. Edge points with an intensity of less than 10% of the maximal intensity are disregarded. The reference WF is stored in the computer for subsequent use. The voltage settings to be assigned to the electrodes of DM2 then have to be found so that the WF of the ATLAS pulse matches the reference WF as closely as possible. This is achieved by application of a closed loop. The algorithm employed for this purpose is the same as that developed in Ref. 5. The deviations between the actual and the reference WFs are minimized by use of the peak-to-valley optical-path difference as a criterion. Usually, approximately five iterations are needed to decrease the peak-to-valley value from the original 10λ to $\lambda/4$. The voltage settings corresponding to minimal WF distortion are stored. They can be used for hours because of the high thermomechanical stability of the ATLAS and the correspondingly low shot-to-shot fluctuations of the WF. For routine operation of the ATLAS, the closed loop is no longer needed once the WF correction is complete. We can then remove the beam splitter feeding the Shack–Hartmann sensor from the beam line to keep the B integral low. In case of performance deterioration, e.g., because of thermal drift, the whole WF correction procedure, which takes ~ 15 s, has to be redone.

We check the quality of the corrected WF in each target chamber by measuring the fluence patterns in the foci of the $F/3$ off-axis parabolas, using an 8-bit CCD camera and a set of calibrated filters. This combination provides an effective dynamic range of $>10^4$. The focus is viewed at $50\times$ magnification. Because of the 1-mm-diameter pinhole SF2, there can be no energy outside the sensor chip ($6\text{ mm} \times 4\text{ mm}$). Hence, the amount of energy that can possibly be hidden in the pixels showing no direct response is at most 10% of the total pulse energy. In each chamber, we obtain the same result for thousands of shots. With DM1 on and DM2 acting as a plane mirror, we find the multiple-peak fluence pattern depicted in the left-hand part of Fig. 4. The Strehl ratio (for its definition, see Ref. 15) is only ~ 0.04 . However, when DM2 is locked to operation for minimal WFA, we find

a dramatic improvement (Fig. 4, right). A single peak appears that contains 65% of the pulse energy within the diffraction-limited diameter. The mean intensity inside the diffraction-limited diameter is raised by a factor of ~ 20 from $\sim 10^{18}$ to 2×10^{19} W/cm 2 . The Strehl ratio increases to 0.7. The Strehl ratio estimated from the corrected WF with a peak-to-valley optical path difference of $\lambda/4$ is 0.8. The difference in the two ratios is attributed to the fact that the real WF has higher-order aberrations that are not measurable with our Shack–Hartmann sensor and are not correctable with our adaptive optics.

We have shown that a combination of two DMs can free ultrashort laser pulses from simultaneously present heavy phase and amplitude modulations without any penalty in recompression fidelity and focusability.

This work was supported by the Commission of the European Union (EU) within the framework of the Association Euratom–Max-Planck-Institut für Plasmaphysik and the EU project ADAPTOOL (contract HPRI-CT-1999-50012). K. Witte's e-mail address is klaus.witte@mpq.mpg.de.

References

1. G. Erbert, L. Bass, R. Hackel, S. Jenkins, K. Kanz, and J. Paisner, in *Conference on Lasers and Electro-Optics*, Vol. 10 of 1991 OSA Technical Digest Series (Optical Society of America, Washington, D.C., 1991), pp. 390–391.
2. M. Pittmann, J. Rousseau, L. Notebaert, S. Ferré, J. Chambaret, and G. Cheriaux, in *Conference on Lasers and Electro-Optics*, Vol. 56 of OSA Trends in Optics and Photonics Series (Optical Society of America, Washington, D.C., 2001), p. 83.
3. S. Backus, R. Bartels, S. Thompson, R. Dollinger, H. Kapteyn, and M. Murnane, *Opt. Lett.* **26**, 465 (2001).
4. B. Van Wonterghem, J. Murray, J. Campbell, D. Speck, C. Barker, I. Smith, D. Browning, and W. Behrend, *Appl. Opt.* **36**, 4932 (1977).
5. K. Akaoka, S. Harayama, K. Tei, Y. Marayuma, and T. Arisawa, *Proc. SPIE* **3265**, 219 (1997).
6. F. Druon, G. Cheriaux, J. Faure, J. Nees, M. Nantel, A. Maksimchuk, J. Chanteloup, and G. Vodvin, *Opt. Lett.* **23**, 1043 (1998).
7. J. Chanteloup, H. Baldis, A. Migus, G. Mourou, B. Loiseaux, and J. Huignard, *Opt. Lett.* **23**, 475 (1998).
8. K. Nemoto, T. Fujiti, and N. Goto, *Proc. SPIE* **2119**, 155 (1994).
9. G. Roger, *J. Phys. Colloq.* **41**, 399 (1980).
10. K. Li You, Q. C. Dong, and W. D. Xiang, *High-Power Laser Particle Beams* **12**, 665 (2000).
11. A. Tokovinin, M. Le Louarn, E. Viard, N. Hubin, and R. Conan, *Astron. Astrophys.* **378**, 710 (2001).
12. K. Yamakawa, P. Chin, A. Magano, and J. Kmetec, *IEEE J. Quantum Electron.* **37**, 2698 (1994).
13. DM1 and DM2 were produced in the mainframe of Max-Planck-Institut–ILIT RAS collaboration. See also J. Dainty, A. Koryabin, and A. Kudryashov, *Appl. Opt.* **37**, 4663 (1998).
14. Z. Wang, Z. Xu, and Z.-Q. Zhang, *IEEE J. Quantum Electron.* **37**, 1 (2001).
15. W. J. Smith, *Modern Optical Engineering*, 2nd ed. (McGraw-Hill, New York, 1990), p. 337.